Generalized geometric criteria for the absence of effective many-body interactions in the Asakura–Oosawa model ⊘

René Wittmann ✉ ⓘD ; Sabine Jansen ⓘD ; Hartmut Löwen ⓘD

Check for updates

View Online Export Citation CrossMark

Articles You May Be Interested In

Generalized geometric criteria for the absence of effective many-body interactions in the Asakura–Oosawa model

René Wittmann,[1,a] 🆔 Sabine Jansen,[2,b] 🆔 and Hartmut Löwen[1,c] 🆔

AFFILIATIONS

[1] Institut für Theoretische Physik II: Weiche Materie, Heinrich-Heine-Universität Düsseldorf, 40225 Düsseldorf, Germany
[2] Mathematisches Institut, Ludwig-Maximilians-Universität München, 80333 Munich, Germany and Munich Center for Quantum Science and Technology (MCQST), Schellingstr. 4, 80799 München, Germany

[a] Author to whom correspondence should be addressed: rene.wittmann@hhu.de
[b] Electronic mail: jansen@math.lmu.de
[c] Electronic mail: hlowen@hhu.de

ABSTRACT

We investigate variants of the Asakura–Oosawa (AO) model for colloid-polymer mixtures, represented by hard classical particles interacting via their excluded volume. The interaction between the polymers is neglected but the colloid-polymer and colloid-colloid interactions are present and can be condensed into an effective depletion interaction among the colloids alone. The original AO model involves hard spherical particles in three spatial dimensions with colloidal radii R and the so-called depletion radius δ of the polymers, such that the minimum possible center-to-center distance between polymers and colloids allowed by the excluded-volume constraints is $R + \delta$. It is common knowledge among physicists that there are only pairwise effective depletion interactions between the colloids if the geometric condition $\delta/R < 2/\sqrt{3} - 1$ is fulfilled. In this case, triplet and higher-order many body interactions are vanishing and the equilibrium statistics of the binary mixture can exactly be mapped onto that of an effective one-component system with the effective depletion pair-potential. Here we rigorously prove that the criterion $\delta/R < 2/\sqrt{3} - 1$ is both sufficient and necessary to guarantee the absence of triplet and higher-order many body interactions among the colloids. For an external hard wall confining the system, we also include a criterion which guarantees that the system can be exactly mapped onto one with effective external one-body interactions. Our general formulation also accounts for polydisperse mixtures and anisotropic shapes of colloids in any spatial dimension. In those cases where the resulting condition is only sufficient, we further demonstrate how to specify improved bounds.

Published under an exclusive license by AIP Publishing. https://doi.org/10.1063/5.0125536

I. INTRODUCTION

Mixtures of classical particles establish not only important model systems of statistical mechanics[1–13] but are also used to a large extent to describe colloidal and colloid–polymer mixtures.[14–22] One of the most famous models is that originally proposed by Asakura and Oosawa.[23–26] This Asakura–Oosawa (AO) model, which is also called Asakura–Oosawa–Vrij model,[27] involves a binary mixture of a big particle species of radius R, representing the colloids, and a small one, representing the polymers (or depletants), which interact solely by excluded volumes. In detail, the minimal distance that the centers of two colloids can approach is given by $2R$, where $R > 0$ is the particle radius. Therefore, the colloids are often in common physical terms referred to as hard spheres. The polymers are ideal, i.e., they do not interact among each other. However, the interaction between the colloids and the polymers is characterized by an additional nonzero depletion radius $\delta > 0$ of the polymers, which ensures that the minimal distance that the centers of a colloid and a polymer particle can approach is given by $R + \delta$. Or, in other words, around the big colloids there is a spherical excluded volume region which is depleted by small polymers as their probability to stay there is zero.
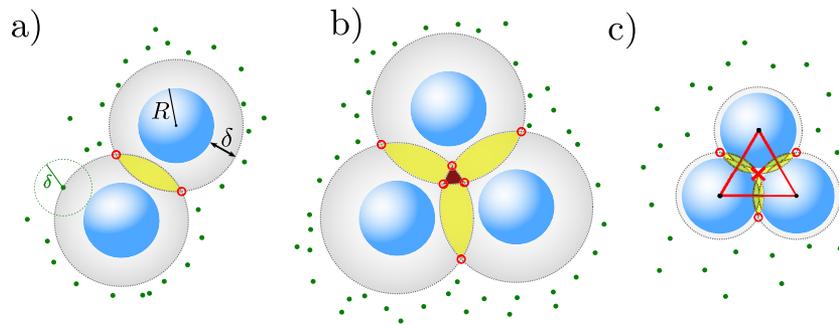
FIG. 1. Schematic of colloids modeled as large hard spheres (blue) of radius R, Eq. (2.1), in the presence of polymers (or depletants), modeled as ideal point particles (green dots), Eq. (2.2), with a depletion radius δ such that the centers of the depletants are excluded from the depletion shells (gray) of radius $R + \delta$ around each colloid, Eq. (2.3). For the purpose of illustration, we draw a dashed green depletion circle around one depletant which is at the smallest possible distance to a colloid. The free volume for the centers of the polymers can be increased when the depletion shells of the colloids intersect (an overlap of the hard cores of the colloids is forbidden). Here we highlight the regions of pair overlap (yellow) and triple overlap (red) of the depletion shells and the points of pair overlap (red circles) and triple overlap (red cross) of their surfaces for different configurations and depletion radii δ. (a) Pairwise intersection of two depletion shells. The volume of the overlap region gives rise to the effective depletion pair potential $V_{cc}^{eff}(r)$ between the colloids, given by Eqs. (2.4) and (2.5). (b) Triple intersection of three depletion shells. The corresponding effective depletion triplet potential is not exactly known. (c) Critical configuration with three spheres at mutual contact and maximal depletion radius $\delta = \delta_{cr}$, such that the depletion shells overlap in a single point. The value of δ_{cr} can be easily inferred from the drawn equilateral triangle $\mathcal{T}$ (red) and leads to the condition (2.6) for the absence of triplet interactions, such that the description of the colloid–colloid interaction by $V_{cc}^{eff}(r)$ becomes exact.

The AO model constitutes a paradigm for coarse-graining a binary mixture towards an effective one-component system by integrating out the degrees of freedom of the small particles.[28,29] This culminates by the important concept of depletion attraction between the colloids as induced by the osmotic pressure of the non-adsorbing polymer coils (the small particles).[14,15] For a pair of colloidal particles this effective depletion attraction can be calculated analytically and equals the overlap volume of the two spherical depletion regions around the colloids times the osmotic polymer pressure. Taking the inverse route, this coarse-graining scheme also allows to efficiently treat pairwise attractions in a one-component system by evaluating a (usually more accurate) theory for mixtures.[30,31] Moreover, an AO mixture in contact with a planar external hard wall can be mapped on a one-component system with additional effective one-body external interactions, as previously considered for wetting and layering situations.[32–38] Also several generalized depletion scenarios involving polydisperse mixtures or anisotropic shapes of the depleted colloids have been investigated.[39–46]

The most remarkable aspect of the AO model that has been established in the physics literature[28,47–49] is that for $\delta/R < 2/\sqrt{3} - 1$ the depletion zones of any statistically possible configuration of the spherical colloids *never* possess a triple (or higher order) overlap. This implies that the effective triplet and higher-order effective interactions between the colloids[50–55] do vanish when integrating out the polymers. This important statistical feature shows that there exists an exact mapping onto an effective one-component system of colloids which then only interact via effective depletion pair-interactions if the depletion zone is sufficiently small. Hence the full AO system can be effectively viewed as a pairwise system interacting via the hard-core repulsion of the colloids plus attractive tail potential defined by the depletion interaction due to the presence of "polymers." For these systems, standard liquid state theory can be applied to obtain static correlation functions and equilibrium phase transitions.[56]

Despite the fundamental importance of depletion interactions in physics, a rigorous proof of the heuristic arguments for the absence of effective higher-order interactions has been missing so far. A mathematical proof should not only confirm the physical intuition, but it often generalizes the known results and more importantly, it sometimes even stimulates new methods and research questions (as, e.g., in the celebrated proof of Kepler's conjecture on the optimal hard-sphere packing[57]), or it helps to uncover loopholes (as, e.g., in the case of quasicrystals[58]).

The aim of this paper is fivefold. First, we prove that the geometric criterion $\delta/R < 2/\sqrt{3} - 1$ for the absence of effective triplet interactions in the standard AO model with identical and spherical colloids is indeed both necessary and sufficient in a strict mathematical sense, by explicitly taking into account all possible configurations. Second, we prove the equally intuitive, but less well known geometric criterion $\delta/R < 1/4$ for the absence of effective external pair interactions for an AO mixture in contact with a planar external hard wall. Third, we elaborate how to establish according criteria for more general AO-type systems, where the basic question of an exact mapping onto a pure pairwise model was not yet much addressed in the literature. To this end, our necessary and sufficient criteria are formulated to also account for polydisperse colloids with different radii in arbitrary spatial dimensions, while we also prove related conditions that are sufficient for non-spherical colloids. Fourth, we discuss in detail whether or not our criteria are optimal for general particle shapes and demonstrate that our developed mathematical toolbox can be used to devise improved implicit bounds. Fifth, by discussing all rigorous results once more in physical terms, we provide an encyclopedia for the various depletion problems covered by our criteria.

This paper is structured as follows. In Sec. II we introduce the AO model in physical terms and briefly state the conditions for the absence of triplet depletion interactions known in the physics literature. In Sec. III we switch to a mathematical language and state our main theorems, providing a rigorous and generalized set of conditions for the absence of triplet depletion interactions. The proof of these theorems is completed in Sec. IV by making contact with the historical Apollonius problem and Descartes' circle theorem. Finally, in Sec. V, we restate the implications of our main theorem in physical terms and make some concluding remarks.

II. THE ASAKURA–OOSAWA (AO) MODEL

In its original version, the Asakura-Oosawa (AO) model for colloid–polymer mixtures is defined for monodisperse spherical colloids in three spatial dimensions, modeled as perfectly hard particles and ideal (i.e., non-interacting) polymers, also called depletants, see Fig. 1 for an illustration of the fundamental aspects. The hard-core colloid–colloid interaction is given by the pair potential

$$V_{cc}(r) = \begin{cases} 0 & \text{if} \quad r \geq 2R \\ \infty & \text{if} \quad r < 2R, \end{cases} \tag{2.1}$$

where r is the distance between two colloid centers. The colloidal interaction radius $R > 0$ sets a typical length scale, such that there is no geometric overlap between the two spheres for $r < 2R$. The infinite pair potential implies a vanishing Boltzmann factor $\exp(-V_{cc}(r)/(k_B T))$, where k_B is the Boltzmann constant and T denotes the temperature, in the classical partition sum so that the statistical weight is zero for any overlapping configuration of these hard spheres. In other words, the particles will not overlap. The polymer–polymer interaction potential

$$V_{pp}(r) = 0, \tag{2.2}$$

corresponds to a vanishing interaction radius, which means that the polymers are treated as point particles. The essential cross-interaction between the colloids and polymers is pairwise and given by the hard-core pair interaction potential

$$V_{cp}(r) = V_{pc}(r) = \begin{cases} 0 & \text{if} \quad r \geq R + \delta \\ \infty & \text{if} \quad r < R + \delta \end{cases} \tag{2.3}$$

with r now denoting the distance between a colloid and polymer center. This interaction introduces the radius $\delta > 0$ of the depletion shell, which is the minimal distance a polymer can approach the spherical surface of the colloid. The case $\delta = 0$ corresponds to an ordinary mixture without any depletion interactions.

The crucial idea behind the AO model is that one can integrate out the degrees of freedom associated with the polymer coordinates and then consider an effective colloid–colloid interaction. This depletion interaction reflects the increase in the free volume accessible to the polymer centers, which is the overall system volume minus the total depletion zone arising from all colloidal particles in the system, if the depletion shells of nearby colloids overlap. Considering the lens-shaped overlap region of two spherical depletion shells in three spatial dimensions, as illustrated in Fig. 1(a), it can be shown exactly that the effective depletion pair potential between two colloids with center-to-center distance r reads

$$V_{cc}^{eff}(r) = V_{cc}(r) + V_{cc}^{dep}(r) \tag{2.4}$$

with the negative contribution

$$V_{cc}^{dep}(r) = \begin{cases} -P_p \dfrac{4\pi(R+\delta)^3}{3}\left(1 - \dfrac{3r}{4(R+\delta)} + \dfrac{r^3}{16(R+\delta)^3}\right) & \text{if } 2R \leq r \leq 2R + 2\delta \\ 0 & \text{else} \end{cases} \tag{2.5}$$

due to depletion if two colloids are sufficiently close such that their depletion shells overlap. The strength of this depletion interaction depends on the osmotic pressure $P_p = k_B T \rho_p$ of the polymers at density ρ_p.

For a triplet configuration of spheres, as shown in Fig. 1(b), the essential point is how exactly the individual depletion shells, which are inaccessible for the polymers, overlap. If there is a region of triple intersection of three depletion shells, then the volume of the overall depletion zone cannot be calculated from the individual depletion shells and their pair overlaps alone. In the language of statistical mechanics[56] this implies that effective many-body interaction between the colloids are arising in addition to the effective pair potential $V_{cc}^{eff}(r)$. In turn, if for *any* configuration of three and more colloids there exists no point where all of their depletion shells do intersect, then triplet and higher many-body interactions do vanish. This reduces the condition for the absence of triplet interactions to a pure geometric overlap problem. In the special situation of monodisperse hard spheres of the same radius R, as considered so far, the geometric criterion for the depletion radius reads[28,47–49]

$$\frac{\delta}{R} < \frac{2}{\sqrt{3}} - 1, \tag{2.6}$$

so that a triple overlap of the depletion shells is excluded for any configuration of three spheres. It can be inferred from the configuration, shown in Fig. 1(c), where the three spheres are at mutual contact. Moreover, if the spheres are at contact with a hard planar external wall, the criterion for the absence of pairwise depletion interactions between the colloids and the wall reads[33,49]

$$\frac{\delta}{R} < \frac{1}{4}. \tag{2.7}$$

The importance of the bound from Eq. (2.6), which implies the condition in Eq. (2.7), stems from the exactness of the AO model, i.e., describing the colloidal degrees of freedom only by the pairwise effective depletion potential, Eq. (2.4), if δ is below the given threshold.

This basic AO model for monodisperse hard spheres can be generalized towards hard hyperspheres (balls) in arbitrary spatial dimensions $n \in \mathbb{N}$ in a straightforward manner by taking for r the Euclidean distance in arbitrary dimensions. Moreover, it can be generalized to arbitrarily shaped hard colloidal bodies in the following way: if – for a given configuration of colloids – the volumes of the two bodies overlap, the pair potential V_{cc} is formally infinite so that overlap is excluded. The polymer–colloid interaction is infinity if the polymer center is closer than the depletion distance δ to at least one point of the colloidal surfaces. In three spatial dimensions, this generalization includes polydisperse colloidal hard spheres with different radii R_i and therefore also a planar hard wall in the limit where one of these radii diverges. It also includes nonspherical shapes, both convex and nonconvex.

We are particularly interested in the following questions. Why is the arrangement of three hard spheres depicted in Fig. 1(c) the critical one, which gives rise to the upper bound for the depletion radius stated in Eq. (2.6)? What is the critical configuration if we consider mixtures with different radii? How must Eq. (2.6) be generalized in such a case, or in general, for arbitrary mixtures of different hard bodies with an anisotropic shape? To answer these questions in a mathematically rigorous way, we extend the problem and consider an arbitrary but fixed arrangement of three balls, for which we seek the maximal shell radius δ_{max}, such that the triple overlap of the depletion shells is exactly in one point, which implies the general condition $\delta < \delta_{max}$. As illustrated in Fig. 2, the definition of δ_{max} depends on the configuration. In what follows, we define δ_{max} in a formal way and analyze its configurational dependence in mathematical terms to determine its minimal value among all possible configurations, which provides both generalized conditions for the absence of triplet interactions and a rigorous proof thereof.
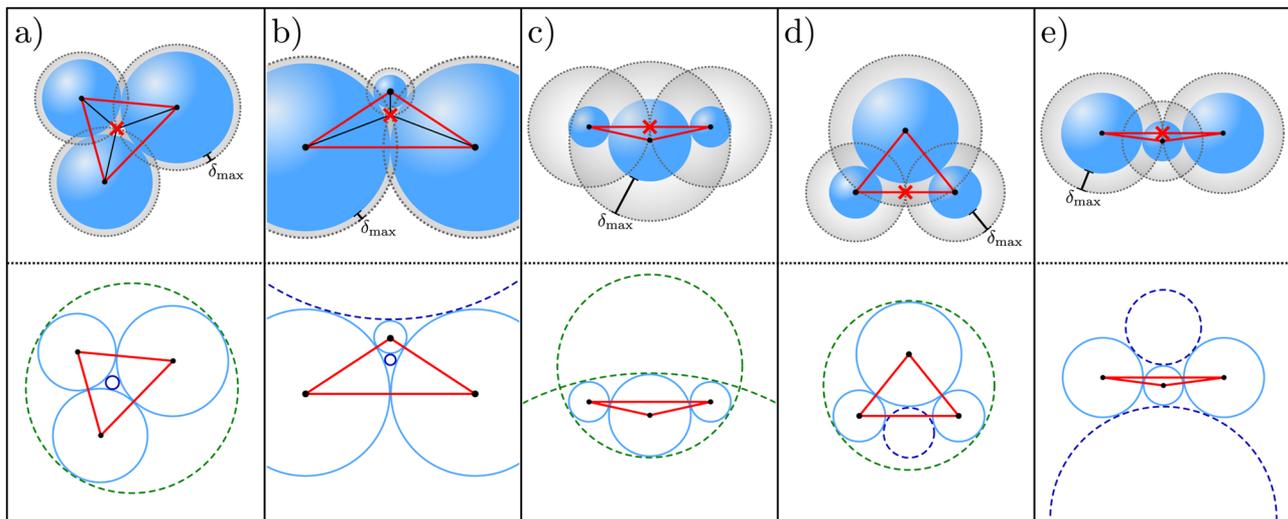
FIG. 2. Illustration of how to determine the maximal depletion radius $\delta_{max} > 0$ around three balls with different radii R_i, such that there is no triple intersection for $\delta < \delta_{max}$. We show a projection of five representative configurations onto a plane containing the triangle $\mathcal{T}$ (red) whose corners are centers of the balls (more details are given in Fig. 3). The balls can thus be treated as two-dimensional disks. **Top panel**: location of the single point **p** of triple intersection (red cross) of the depletion zones (gray) of the three disks (blue) with total radii $R_i + \delta_{max}$, compare Proposition 4.1. **Bottom panel**: (segments of) solution circles of the related Apollonius problem, posed in the specific form to find a circle (dark blue) that is externally tangent to the three given circles (light blue) which are mutually externally tangent. Internally tangent solution circles (dark green) have no relevance for the depletion problem. The center of a solution circle represents the point **p** (and its radius $\delta^* = \delta_{max}$ equals the maximal depletion radius) if and only if it is located inside the triangle $\mathcal{T}$ (red) and the circle is externally tangent, compare Proposition 4.1. These circles are drawn with solid lines, all other solutions with dashed lines. The columns depict a representative scenario with (a) one externally tangent solution circle with center inside $\mathcal{T}$; (b) two externally tangent solutions, exactly one circle has its center inside $\mathcal{T}$; (c) no externally tangent solutions; (d) one externally tangent solution circle with center outside $\mathcal{T}$; (e) two externally tangent solution circles with both centers outside $\mathcal{T}$.

III. CONDITIONS FOR THE ABSENCE OF TRIPLET INTERACTIONS

Our main mathematical result is a sufficient condition for the absence of triple overlap of dilated versions of non-overlapping convex bodies in $\mathbb{R}^n$ with $n \geq 2$. By "non-overlapping" we mean that the interiors of the convex bodies are disjoint; contact in boundary points is allowed. Given $\delta > 0$ and $C \subset \mathbb{R}^n$, consider the dilated set (often called *outer parallel body*) given by

$$C(\delta) = \{\mathbf{r} \in \mathbb{R}^n : \text{dist}(\mathbf{r}, C) \leq \delta\}, \tag{3.1}$$

where the distance of a point to a set is defined in terms of the Euclidean distance $|\cdot|$ as $\text{dist}(\mathbf{r}, C) = \inf_{\mathbf{y} \in C} |\mathbf{y} - \mathbf{r}|$.

The sufficient condition for absence of triple overlap involves a bound on the rolling radius of the (non-dilated) sets. A closed convex set C has positive rolling radius if a ball can roll freely inside C along the boundary, i.e., if for some radius $r > 0$ and all $\mathbf{y} \in \partial C$ there exists a closed ball $B(\mathbf{x}, r)$ with $\mathbf{y} \in B(\mathbf{x}, r) \subset C$. The *rolling radius* $\text{Roll}(C)$ is the supremum of the possible radii $r > 0$. If no ball with radius $r > 0$ can roll freely inside C, we assign $\text{Roll}(C) = 0$.

Remark 3.1. When ∂C is a C^2 surface, Blaschke's rolling theorems[59] (see also Ref. 60 for extensions and additional references) show that the rolling radius is the minimum of the inverse of the principal curvatures. When smoothness of the boundary ∂C is not assumed, curvature in convex geometry can be defined in terms of curvature measures. Bounded curvature is replaced with absolute continuity of the curvature measure with respect to a surface measure and the condition that the Radon-Nikodym derivative is finite; a relation with strictly positive rolling radius can be established in this general context as well.[61–63]

Theorem 3.2. Fix $n \geq 2$ and $\kappa \geq 3$. Let C_i, $i = 1, 2, \ldots, \kappa$ be compact convex subsets of $\mathbb{R}^n$ with disjoint interiors. Suppose that they have positive rolling radii $\text{Roll}(C_i) > 0$ and that

$$\delta < \left(\frac{2}{\sqrt{3}} - 1\right) \min_{i=1,\ldots,\kappa} \text{Roll}(C_i). \tag{3.2}$$

Then the intersection of the dilated sets is empty: $\bigcap_{i=1}^{\kappa} C_i(\delta) = \emptyset$. If instead

$$\delta \leq \left(\frac{2}{\sqrt{3}} - 1\right) \min_{i=1,\ldots,\kappa} \text{Roll}(C_i) \tag{3.3}$$

then the intersection has empty interior and zero Lebesgue measure: $\text{vol}\left(\bigcap_{i=1}^{\kappa} C_i(\delta)\right) = 0$.

Theorem 3.2 is complemented at the end of this section by a result when one of the C_i's is a half-plane ("hard wall"), see Theorem 3.11.

In the situation of condition (3.3) we shall say that *there is no overlap* or that *there is no triplet (or higher-order) interaction*. This is because effective interactions are given by volumes of intersections and may vanish even if the intersection is non-empty, e.g., when it consists of a single point.

Theorem 3.2 is a consequence of the following theorem on triple overlap of dilation of closed balls, which also provides a necessary criterion in this special case.

Theorem 3.3. Fix $n \geq 2$ and $R > 0$. The following two conditions are equivalent:

(i) $\delta > 0$ and $R > 0$ satisfy

$$\delta < \left(\frac{2}{\sqrt{3}} - 1\right) R. \tag{3.4}$$

(ii) For all closed balls $B(\mathbf{r}_i, R_i) \subset \mathbb{R}^n$, $i = 1, 2, 3$ with $R_i > 0$ and centers $\mathbf{r}_i \in \mathbb{R}^n$ that have disjoint interiors and satisfy $\min(R_1, R_2, R_3) \geq R$, the dilated balls $B(\mathbf{r}_i, R_i + \delta)$ have empty triple intersection.

Before we address the Proof of Theorem 3.3, let us show how Theorem 3.2 follows. In fact, it is enough to know the implication (i) $\Rightarrow$ (ii) from Theorem 3.3 for balls that have the same radius R.

Proof of Theorem 3.2. Consider first triple intersection, $\kappa = 3$. We show that if the triple overlap is non-empty, then the condition on δ is violated. Thus, suppose that there exists a point $\mathbf{r} \in \mathbb{R}^n$ that is in the triple intersection of the dilations $C_i(\delta)$, $i = 1, 2, 3$. Let $\mathbf{p}_i$ be the projection of $\mathbf{r}$ onto C_i, i.e., the uniquely defined point $\mathbf{p}_i \in C_i$ with $|\mathbf{r} - \mathbf{p}_i| = \text{dist}(\mathbf{r}, C_i) \leq \delta$. Set $R_{\min} := \min_{i=1,2,3} \text{Roll}(C_i)$. If $\mathbf{r}$ is in none of the interiors of the C_i's, then $\mathbf{p}_i \in \partial C_i$ and the definition of the rolling radius guarantees the existence of three balls $B(\mathbf{x}_i, R_{\min})$ such that $\mathbf{p}_i \in B(\mathbf{x}_i, R_{\min}) \subset C_i$ for $i = 1, 2, 3$. The three balls of radius $R_{\min}$ have disjoint interiors and the triple intersection $\bigcap_{i=1}^{3} B(\mathbf{x}_i, R_{\min} + \delta)$ is non-empty as it contains $\mathbf{r}$. Theorem 3.3 with $R_i = R_{\min}$ implies that $\delta \geq (2/\sqrt{3} - 1)R_{\min}$.

Now suppose $\mathbf{r}$ is in the interior of one of the C_i's, say C_1. By the disjointness of the interiors of the sets C_i, the point $\mathbf{r}$ is not in the interior of C_2 or C_3, and we can define the projections $\mathbf{p}_i \in \partial C_i$ for $i = 2, 3$ and the associated balls $B_i = B(\mathbf{x}_i, R_{\min})$, $i = 2, 3$ as before.

We claim that there is also a closed ball $B_1' \subset C_1$ of radius $R_{\min}$ that contains $\mathbf{r}$. To see why, consider the set of all balls that contain $\mathbf{r}$ and are contained in C_1, and among them let $B(\mathbf{x}_1, R)$ be a ball of maximum possible radius. Then $B(\mathbf{x}_1, R)$ touches the boundary ∂C_1 in at least one point $\mathbf{p}_1$. Working with the boundary point $\mathbf{p}_1$ and the definition of the rolling radius one sees that R must be larger or equal to the rolling radius R_1 of C_1, hence $R \geq R_1 \geq R_{\min}$. In particular, there exists a ball $B_1' \subset B(\mathbf{x}_1, R) \subset C_1$ of radius $R_{\min}$ with $\mathbf{r} \in B_1'$.

The balls B_1', B_2, B_3 have disjoint interiors and their δ-dilations contain $\mathbf{r}$, we conclude again with Theorem 3.3 applied to $R_i = R_{\min}$ that $\delta \geq (2/\sqrt{3} - 1)R_{\min}$. This completes the proof of empty intersection for $\kappa = 3$. The claim for $\kappa \geq 3$ follows right away since the intersection $\cap_{i=1}^\kappa C_i(\delta)$ is contained in the triple intersection $\cap_{i=1}^3 C_i(\delta)$.

For the second part of the theorem the only case left to investigate is when δ is equal to the right-hand side of condition (3.3). A continuity argument shows that the convex set $\cap_{i=1}^\kappa C_i(\delta)$ has empty interior: the interior consists of those points $y \in \mathbb{R}^n$ that have distance strictly smaller than δ to each of the sets C_i. Every such point is in the intersection $\cap_{i=1}^\kappa C_i(\delta')$ for some $\delta' < \delta$. As the latter intersection is empty by the part of the theorem already proven, no such point exists and the interior is empty. The only way for a convex set to have empty interior is that the convex set is contained in some affine hyperplane, in which case the measure is zero. $\qquad\square$

Remark 3.4. A close look at the proof reveals that convexity and compactness are not essential for Theorem 3.2: If, for some radius $R > 0$, each C_i has the property that every point $\mathbf{p} \in C_i$ is contained in a ball of radius R that lies entirely in C_i [for convex bodies, this implies $R \leq \min_{i=1,\ldots,\kappa} \mathrm{Roll}(C_i)$], and δ satisfies condition (3.4) for this R, then the dilated bodies $C_i(\delta)$ have empty intersection.

The bound in Theorem 3.2 can be improved for some compact convex sets with nonempty interior, specifically for the case of convex polyhedra with $\mathrm{Roll}(C_i) = 0$.

Proposition 3.5. Fix $n \geq 2$ and $\kappa \geq 3$. Let C_i, $i = 1, 2, \ldots, \kappa$ be compact convex subsets of $\mathbb{R}^n$ with disjoint interiors. For any convex and compact subset $K_i \subseteq C_i$ with $\mathrm{Roll}(K_i) > 0$, we define

$$\Delta_{K_i} := \left(\frac{2}{\sqrt{3}} - 1 \right) \mathrm{Roll}(K_i). \tag{3.5}$$

Let us further define $\Delta^*(K_i) := \sup \{ \delta' \geq 0 : C_i(\delta') \subseteq K_i(\Delta_{K_i}) \}$ *and subsequently* $\Delta_i^* := \sup_{K_i \subseteq C_i} \Delta^*(K_i)$*. Then the condition*

$$\delta < \min_{i=1,\ldots,\kappa} \Delta_i^* = \min_{i=1,\ldots,\kappa} \sup_{K_i \subseteq C_i} \sup \{ \delta' \geq 0 : C_i(\delta') \subseteq K_i(\Delta_{K_i}) \} \tag{3.6}$$

implies that $\cap_{i=1}^\kappa C_i(\delta) = \emptyset$.

Proof. By definition, all $K_i \subseteq C_i$ have disjoint interiors. Then, it follows by Theorem 3.2 that the intersection of the dilated sets $K_i(\Delta)$ is empty if the pseudo-depletion radius Δ satisfies $\Delta < \min_{i=1,\ldots,\kappa} \Delta_{K_i}$. Now choose a depletion radius δ' with $0 \leq \delta' \leq \min_{i=1,\ldots,\kappa} \Delta_{K_i}$ such that $C_i(\delta') \subseteq K_i(\Delta_{K_i})$ for all $i = 1, 2, \ldots, \kappa$, then also the intersection of all dilated sets $C_i(\delta')$ has empty interior. Therefore, any choice of such a δ' implies the assertion $\cap_{i=1}^\kappa C_i(\delta) = \emptyset$ for $\delta < \delta'$. The optimal choice of such a δ' is specified in Eq. (3.6), where $\Delta^*(K_i)$ denotes the optimal radius for given convex and compact subsets K_i, while Δ_i^* involves the optimization over all K_i. $\qquad\square$

It is obvious that the bound in Eq. (3.6) is better or equal to that in Eq. (3.2), since the bounds are equal if the supremum is attained for $K_i = C_i$ in case of the C_i with the smallest rolling radius. If one δ' exceeds the bound in Eq. (3.2) we have found an improvement. It remains an open problem whether this improved bound, which is sufficient for the absence of triple intersections, also allows the definition of a necessary criterion in the sense of Theorem 3.3.

For the Proof of Theorem 3.3, we start from three non-overlapping hard bodies and grow the shell radius δ from $\delta = 0$ until the triple intersection first becomes non-empty. This defines a threshold value $\delta_{\max}$ that we compute explicitly when the three bodies are balls in contact. The threshold value is defined precisely in the next lemma, which works for general compact bodies.

Lemma 3.6 (Existence and uniqueness of maximal shell radius for triple intersection). *Let C_i, $i = 1, 2, 3$ be three non-empty compact subsets of $\mathbb{R}^n$ with disjoint interiors. Then there exists a uniquely defined $\delta_{\max} = \delta_{\max}(C_1, C_2, C_3) \in [0, \infty)$ such that the triple intersection of the dilated sets $C_i(\delta)$ is empty if and only if $\delta < \delta_{\max}$:*

$$C_1(\delta) \cap C_2(\delta) \cap C_3(\delta) = \emptyset \iff \delta < \delta_{\max}(C_1, C_2, C_3). \tag{3.7}$$

Proof. The threshold value $\delta_{\max}$ is clearly unique. It remains to prove existence. Let

$$\delta_{\max} := \sup \{ \delta > 0 : C_1(\delta) \cap C_2(\delta) \cap C_3(\delta) = \emptyset \} \tag{3.8}$$

if the latter set is non-empty, and $\delta_{\max} = 0$ otherwise (this may occur when the convex bodies touch in a common cusp of the surfaces ∂C_i). Clearly the triple intersection is non-empty for all sufficiently large δ, therefore $\delta_{\max} < \infty$.

To check that Eq. (3.7) holds true, we note that the map $\delta \mapsto \cap_{i=1}^3 C_i(\delta) =: \mathcal{I}(\delta)$ is monotone increasing, i.e., $\delta \le \delta'$ implies $\mathcal{I}(\delta) \subset \mathcal{I}(\delta')$. Let $\delta < \delta_{\max}$. Then by the definition (3.8) of $\delta_{\max}$ there exists δ' with $\delta \le \delta' \le \delta_{\max}$, such that $\mathcal{I}(\delta') = \emptyset$. The inclusion $\mathcal{I}(\delta) \subset \mathcal{I}(\delta')$ then implies $\mathcal{I}(\delta) = \emptyset$. For $\delta > \delta_{\max}$, we get right away from (3.8) that the triple intersection is non-empty.

It remains to check that at $\delta = \delta_{\max}$, the triple intersection $\mathcal{I}(\delta)$ is non-empty. To that aim let $(\delta_n)_{n \in \mathbb{N}}$ be a strictly decreasing sequence with $\delta_n \downarrow \delta_{\max}$. Let $(\mathbf{x}_n)_{n \in \mathbb{N}}$ be a sequence of points with $\mathbf{x}_n \in \mathcal{I}(\delta_n)$. The sequence $(\mathbf{x}_n)$ is bounded and therefore admits an accumulation point $\mathbf{x}^* \in \mathbb{R}^n$; assume for simplicity that $\mathbf{x}_n \to \mathbf{x}^*$ (if not, pass to a subsequence). By the continuity of the maps $\mathbf{x} \mapsto \mathrm{dist}(\mathbf{x}, C_i)$, the limit point $\mathbf{x}^*$ satisfies

$$\mathrm{dist}(\mathbf{x}^*, C_i) = \lim_{n \to \infty} \mathrm{dist}(\mathbf{x}_n, C_i) \le \lim_{n \to \infty} \delta_n = \delta_{\max}. \tag{3.9}$$

for $i = 1, 2, 3$. As a consequence, $\mathbf{x}^*$ is in $\mathcal{I}(\delta_{\max})$, hence $\mathcal{I}(\delta_{\max})$ is non-empty. It follows that $\delta_{\max}$ defined in (3.8) satisfies (3.7). $\qquad \square$

Next we specialize to convex bodies that are closed balls. For balls it is enough to understand the two-dimensional setup, as depicted in Fig. 2.

Lemma 3.7 (Reduced dimensionality of the overlap problem). *Let $B_i = B(\mathbf{r}_i, R_i)$, $i = 1, 2, 3$ be three closed balls with disjoint interiors and $\mathcal{P} \subset \mathbb{R}^n$ a two-dimensional affine subspace containing the three centers $\mathbf{r}_i$, $i = 1, 2, 3$. Then for all $\delta > 0$,*

$$\bigcap_{i=1}^3 B(\mathbf{r}_i, R_i + \delta) = \emptyset \;\Leftrightarrow\; \mathcal{P} \cap \left(\bigcap_{i=1}^3 B(\mathbf{r}_i, R_i + \delta) \right) = \emptyset. \tag{3.10}$$

Proof. The implication "$\Rightarrow$" is trivial. The converse implication follows once we prove

$$\bigcap_{i=1}^3 B(\mathbf{r}_i, R_i + \delta) \ne \emptyset \;\Rightarrow\; \mathcal{P} \cap \left(\bigcap_{i=1}^3 B(\mathbf{r}_i, R_i + \delta) \right) \ne \emptyset. \tag{3.11}$$

Let $\mathbf{r} \in \cap_{i=1}^3 B(\mathbf{r}_i, R_i + \delta)$ and $\mathbf{r}^\perp$ the orthogonal projection of $\mathbf{r}$ onto the plane $\mathcal{P}$. Then $|\mathbf{r}_i - \mathbf{r}^\perp| \le |\mathbf{r}_i - \mathbf{r}| \le R_i + \delta$, for all $i = 1, 2, 3$. It follows that $\mathbf{r}^\perp$ is in $\mathcal{P} \cap (\cap_{i=1}^3 B(\mathbf{r}_i, R_i + \delta))$, in particular the latter set is non-empty. $\qquad \square$

Thus let us focus on dimension $n = 2$, in which balls turn into disks. Consider first the non-degenerate case in which the three centers $\mathbf{r}_i$ of the non-overlapping disks do not lie on a common line. Let $\mathcal{T}$ be the triangle with corners $\mathbf{r}_i$, $i = 1, 2, 3$. The triangle has interior angles $\alpha_i \in (0, \pi)$ and side-lengths ℓ_i. The indices are such that α_i is the angle at corner i and ℓ_i is the length of the triangle side opposite the corner $\mathbf{r}_i$, see Fig. 3. Non-overlapping of the balls is equivalent to the condition $\ell_i \ge R_j + R_k$ for all pairwise distinct i, j, k.

Given three disks $B_i = B(\mathbf{r}_i, R_i)$, consider the maximal shell radius $\delta_{\max} = \delta_{\max}(B_1, B_2, B_3)$ from Lemma 3.6. At fixed radii R_1, R_2, R_3, it is a function of the triangle $\mathcal{T}$ with corners $\mathbf{r}_i$ that is invariant under Euclidean isometries of the plane. Up to Euclidean transformations, the triangle $\mathcal{T}$ is uniquely determined by fixing an angle α_i and the side lengths ℓ_j, ℓ_k of the adjacent triangle sides. Thus we may view $\delta_{\max}$ as a function of, say, α_1, ℓ_2, and ℓ_3. By some abuse of notation we use the same letter $\delta_{\max}(\alpha_i, \ell_j, \ell_k)$.
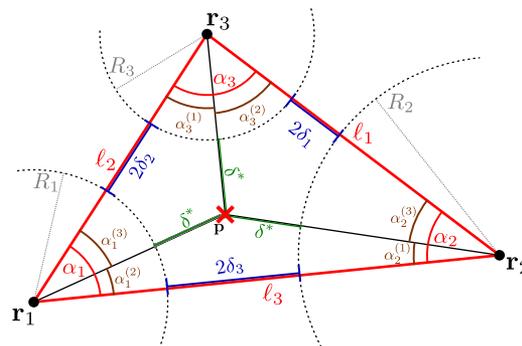
FIG. 3. Geometry of the triangle $\mathcal{T}$ with edge lengths ℓ_i, interior angles α_i and corners at $\mathbf{r}_i$ with $i = 1, 2, 3$, as introduced before Proposition 3.8. The corners correspond to the centers of three disks $B(\mathbf{r}_i, R_i)$ of radii R_i, compare Fig. 2. We also indicate the particular depletion radii δ_i, defined in Eq. (4.1), such that the two dilated disks $B(\mathbf{r}_j, R_j + \delta_i)$ and $B(\mathbf{r}_k, R_k + \delta_i)$ are at contact ($\{i, j, k\} = \{1, 2, 3\}$). When the three dilated disks $B(\mathbf{r}_i, R_i + \delta^*)$ intersect in a single point $\mathbf{p} \in \mathcal{T}$ (red cross), we define the angles $\alpha_i^{(j)}$ with $j \ne i$ according to Eq. (4.10).

Proposition 3.8 (Monotonicity of the maximal shell radius). *Fix* $R_1, R_2, R_3 > 0$. *Then, for all enumerations* (i, j, k) *of* $\{1, 2, 3\}$ *and all* $\ell_j, \ell_k > 0$, *the map*

$$(0, \pi) \ni \alpha_i \mapsto \delta_{\max}(\alpha_i, \ell_j, \ell_k)$$

is monotone increasing.

The proof is given in Sec. IV. The proposition says that the decrease in an angle α_i, at fixed adjacent side lengths results in a decrease (or no change at all) of the maximal shell radius $\delta_{\max}$. Now, every triangle satisfying the hard-core constraints $\ell_i \geq R_j + R_k$, $\{i, j, k\} = \{1, 2, 3\}$, can be mapped to a triangle in which $\ell_i = R_j + R_k$, by a succession of two such angle decreasing moves. The only exception, explicitly treated in the proof of Corollary 3.9 below, is when an inner angle can be decreased until all centers are collinear, without creating any overlap among the balls.

Let

$$\delta_{cr}(R_1, R_2, R_3) = \delta_{\max}\big(B(\mathbf{r}_1', R_1), B(\mathbf{r}_2', R_2), B(\mathbf{r}_3', R_3)\big) \tag{3.12}$$

be the critical shell radius in a configuration of non-overlapping disks that are in contact, i.e., $|\mathbf{r}_i' - \mathbf{r}_j'| = R_i + R_j$ for all distinct $i, j \in \{1, 2, 3\}$. Notice that up to Euclidean isometries of the plane, there is a unique such triangle.

Corollary 3.9 (Critical shell radius for fixed radii). *For all radii* $R_1, R_2, R_3 > 0$, *and all disks* $B(\mathbf{r}_i, R_i) \subset \mathbb{R}^2$, $i = 1, 2, 3$, *that have disjoint interiors, we have*

$$\delta_{\max}(B(\mathbf{r}_1, R_1), B(\mathbf{r}_2, R_2), B(\mathbf{r}_3, R_3)) \geq \delta_{cr}(R_1, R_2, R_3). \tag{3.13}$$

Proof. If the configuration of non-overlapping disks can be turned into a configuration of disks at contact by a sequence of angle-decreasing moves, then the inequality follows from the monotonicity in Proposition 3.8. If the configuration is instead turned into a configuration of non-overlapping disks with collinear centers, corresponding to a degenerate triangle with one angle π and two zero angles, we notice that the monotonicity from Proposition 3.8 extends to the closed interval $[0, \pi]$ by the continuity of the map $\alpha_1 \mapsto \delta_{\max}(\alpha_1, \ell_2, \ell_3)$ and therefore the maximal shell radius $\delta_{\max}$ of the original configuration is still bounded from below by the maximal radius of the aligned disks after decreasing the angle to zero. The latter is easily seen to be larger or equal to the radius of the middle disk, which is clearly larger than the critical radius $\delta_{cr}(R_1, R_2, R_3)$ by the explicit formula provided in Proposition 3.10. Alternatively, to directly arrive at the critical configuration with all three disks in mutual contact, the maximal shell radius for aligned disks can be made smaller by shrinking distances so that the middle one of the aligned disks is in contact with its two neighbors, and then the shell radius is further decreased by decreasing the angle π of the degenerate triangle until we end up with a configuration in which all disks are in contact. □

The critical shell radius δ_{cr} for disks that are in contact is given by an explicit formula. In Sec. IV we prove that it is equal to the radius of the inner Soddy circle,[64] which can be computed with Descartes' circle theorem, see Refs. 65 and 66 and references therein.

Proposition 3.10 (Critical shell radius at contact). *For all* R_1, R_2, R_3, *we have*

$$\delta_{cr}(R_1, R_2, R_3) = \left(R_1^{-1} + R_2^{-1} + R_3^{-1} + 2\sqrt{(R_1 R_2)^{-1} + (R_2 R_3)^{-1} + (R_1 R_3)^{-1}}\right)^{-1}. \tag{3.14}$$

The proposition is proven in Sec. IV by establishing a relation with the Apollonius problem of tangent circles[67] (Chap. VI). Remember that the latter consists in finding a circle that is tangent to three given non-intersecting circles. Descartes' circle theorem concerns the special case where the three given circles in the Apollonius problem are in contact in three different points. This special case is sometimes called four-coins problem.[66]

Proposition 3.10 implies right away that δ_{cr} is strictly increasing in each R_i. In particular, setting $R := \min(R_1, R_2, R_3)$, we get

$$\delta_{cr}(R_1, R_2, R_3) \geq \delta_{cr}(R, R, R) = \left(\frac{2}{\sqrt{3}} - 1\right) R. \tag{3.15}$$

We are now ready to prove Theorem 3.3.

Proof of Theorem 3.3. In view of Lemma 3.7 it is enough to treat the two-dimensional case. Thus let $n = 2$. Suppose that $\delta < \left(\frac{2}{\sqrt{3}} - 1\right) \min(R_1, R_2, R_3)$. Then Eq. (3.15) and Corollary 3.9 yield

$$\delta < \delta_{\max}(B(\mathbf{r}_1, R_1 + \delta), B(\mathbf{r}_2, R_2 + \delta), B(\mathbf{r}_3, R_3 + \delta)). \tag{3.16}$$

By the definition of $\delta_{\max}$ in Lemma 3.6, it follows that the intersection $\cap_{i=1}^3 B(\mathbf{r}_i, R_i + \delta)$ is empty. This proves the implication (i) $\Rightarrow$ (ii).

Now suppose that $\cap_{i=1}^3 B(\mathbf{r}_i, R_i + \delta) = \emptyset$ for all positions $\mathbf{r}_i \in \mathbb{R}^n$. In particular, the relation $\cap_{i=1}^3 B(\mathbf{r}_i', R + \delta) = \emptyset$ also holds for three balls with radius $R = \min(R_1, R_2, R_3)$ at contact, i.e., $|\mathbf{r}_i' - \mathbf{r}_j'| = 2R$ for all distinct $i, j \in \{1, 2, 3\}$. Then the converse implication follows directly from Eq. (3.15) and the uniqueness of δ_{cr}, defined in Eq. (3.12), which is implied in Lemma 3.6. □

27 October 2023 11:53:56

We conclude with a sufficient result on absence of triplet intersections for three bodies C_i, $i = 1, 2, 3$, when one of them, say C_3, is a half-plane, modeling a hard wall. A half-plane may be regarded as a ball with infinite radius. Setting $R := \min(R_1, R_2)$, we get instead of Eq. (3.15)

$$\lim_{R_w \to \infty} \delta_{cr}(R_1, R_2, R_w) \geq \lim_{R_w \to \infty} \delta_{cr}(R, R, R_w) = \frac{R}{4}. \tag{3.17}$$

which leads to the following theorem. By closed half-space we mean a set of the form $\{\mathbf{x} \in \mathbb{R}^n : \mathbf{x} \cdot \mathbf{n} \leq c\}$ for some $\mathbf{n} \in \mathbb{R}^n$ and some constant $c \in \mathbb{R}$.

Theorem 3.11. *Fix $n \geq 2$ and $\kappa \geq 3$. Let C_i, $i = 1, 2, \ldots, \kappa - 1$ be compact convex subsets of $\mathbb{R}^n$ and C_κ a closed half-space. Suppose that the C_i, $i \leq \kappa - 1$ have positive rolling radii $\mathrm{Roll}(C_i) > 0$ and that*

$$\delta < \frac{1}{4} \min_{i=1,\ldots,\kappa} \mathrm{Roll}(C_i). \tag{3.18}$$

Then the intersection of the dilated sets is empty: $\bigcap_{i=1}^{\kappa} C_i(\delta) = \emptyset$. The condition (3.18) with inequality instead of strict inequality is sufficient to guarantee that the intersection has zero volume.

The proof is omitted as it is similar to the proofs of Theorem 3.2 and a version of Theorem 3.3 for two balls and a half-plane, involving the necessary and sufficient condition

$$\delta < \frac{1}{4} R \tag{3.19}$$

for $\delta > 0$ and $R > 0$, such that for all closed balls $B(\mathbf{r}_i, R_i) \subset \mathbb{R}^n$, $i = 1, 2$ with $R_i > 0$ and centers $\mathbf{r}_i \in \mathbb{R}^n$ that have disjoint interiors and satisfy $\min(R_1, R_2) \geq R$ the dilated balls $B(\mathbf{r}_i, R_i + \delta)$ have empty triple intersection.

IV. PROOF OF PROPOSITIONS 3.8 AND 3.10

Throughout this section we work in dimension $n = 2$. The proof of Propositions 3.8 builds on explicit formulas for $\delta_{\max}$, governed by a case distinction. The guiding idea is the following. Fix three non-overlapping disks $B(\mathbf{r}_i, R_i)$, $i = 1, 2, 3$. For very small δ, all pairwise intersections $B(\mathbf{r}_i, R_i + \delta) \cap B(\mathbf{r}_j, R_j + \delta)$, $i \neq j$, vanish. As δ increases, typically at some point one of the pairwise intersections becomes non-empty, then another one, and finally all three of them. Once all three of them are non-empty, there are two possibilities: either the regions of pairwise intersection in turn intersect among themselves, or they do not. In the first case the region of triple intersection is in fact non-empty and we have found $\delta_{\max}$. In the second case we need to increase δ further before we reach $\delta_{\max}$; we shall see that in this case, $\delta_{\max}$ is the radius of one of the Apollonius circles.

To avoid burdensome considerations of borderline cases, we assume throughout this section that the centers $\mathbf{r}_i$, $i = 1, 2, 3$ are not collinear (i.e., they do not lie on a common line). We note, however, that the results extend to collinear centers as well if we allow for degenerate triangles with angles $\alpha_i = 0$, $\alpha_j = 0$ and $\alpha_k = \pi$. These cases are accounted for in Corollary 3.9.

A. Critical shell radius vs Apollonius circles

Remember the angles α_i and the side lengths ℓ_i of the triangle $\mathcal{T}$ with corners $\mathbf{r}_i$, $i = 1, 2, 3$, see Fig. 3. For $\{i, j, k\} = \{1, 2, 3\}$, set

$$\delta_i := \frac{1}{2}(\ell_i - R_k - R_j) \geq 0. \tag{4.1}$$

Clearly

$$B(\mathbf{r}_j, R_j + \delta) \cap B(\mathbf{r}_k, R_k + \delta) \neq \emptyset \iff \delta \geq \delta_i. \tag{4.2}$$

We may label the corners of the triangle in such a way that the thresholds δ_i for pairwise intersections are ordered as

$$\delta_1 \leq \delta_2 \leq \delta_3. \tag{4.3}$$

If the triple intersection $\cap_{i=1}^{3} B(\mathbf{r}_i, R_i + \delta)$ is non-empty, then necessarily all pairwise intersections are non-empty, therefore $\delta_{\max} = \delta_{\max}(B(\mathbf{r}_1, R_1 + \delta), B(\mathbf{r}_2, R_2 + \delta), B(\mathbf{r}_3, R_3 + \delta))$ satisfies

$$\delta_{\max} \geq \max(\delta_1, \delta_2, \delta_3) = \delta_3. \tag{4.4}$$

The main result of this subsection is the following dichotomy.

Proposition 4.1. Let $B(\mathbf{r}_i, R_i)$, $i = 1, 2, 3$ be three disks in $\mathbb{R}^2$ with pairwise disjoint interiors and non-collinear centers. Then, either one or the other of the following two cases occurs:

1. There exists a circle $\partial B(\mathbf{p}, \delta^*)$ centered in the interior of the triangle $\mathcal{T}$ with $|\mathbf{p} - \mathbf{r}_i| = R_i + \delta^*$ for $i = 1, 2, 3$, in particular the circle is externally tangent to the three circles $\partial B(\mathbf{r}_i, R_i)$. We have

$$\delta_{\max} = \delta^* > \max(\delta_1, \delta_2, \delta_3) \tag{4.5}$$

and the triple intersection $\cap_{i=1}^{3} B(\mathbf{r}_i, R_i + \delta_{\max})$ is the singleton $\{\mathbf{p}\}$.

2. There is no such circle, $\delta_{\max}$ is equal to $\max(\delta_1, \delta_2, \delta_3)$ and the triple intersection is a single point $\mathbf{p}$ on the boundary of the triangle.

The location of the triple intersection for the maximal depletion radius $\delta_{\max}$ is drawn in the top panel of Fig. 2 for a range of selected configurations of three disks. In case 1, the shell radius δ^* is the radius of one of the Apollonius circles[67] (Chap. VI). Note that our circle from case 1 is uniquely defined while the Apollonius problem may have up to eight solution circles, roughly because tangency merely requires $|\mathbf{p} - \mathbf{r}_i| = \pm(R_i + \delta^*)$, while the expression on the right-hand side must be positive (a minus sign of R_i or δ^* corresponds to internal tangency which is not relevant here). Furthermore, in case 2, there might very well be an Apollonius circle whose center satisfies the appropriate conditions $|\mathbf{p} - \mathbf{r}_i| = R_i + \delta^*$ for all i, but that center is not in the interior of the triangle. The relation between our depletion problem and the Apollonius circles is also illustrated in the bottom panel of Fig. 2.

Lemma 4.2. If $\delta_{\max} = \delta_3 = \max(\delta_1, \delta_2, \delta_3)$, then the triple intersection $\cap_{i=1}^{3} B(\mathbf{r}_i, R_i + \delta_{\max})$ at maximal shell radius $\delta = \delta_{\max}$ is equal to the pairwise intersection $\cap_{i=1}^{2} B(\mathbf{r}_i, R_i + \delta_{\max})$ and consists of a single point $\mathbf{p}$ on the triangle side connecting $\mathbf{r}_1$ and $\mathbf{r}_2$. The point $\mathbf{p}$ satisfies

$$|\mathbf{p} - \mathbf{r}_1| = R_1 + \delta_{\max}, \quad |\mathbf{p} - \mathbf{r}_2| = R_2 + \delta_{\max}, \quad |\mathbf{p} - \mathbf{r}_3| \le R_3 + \delta_{\max} \tag{4.6}$$

Proof. At $\delta = \delta_3$ the intersection $\cap_{i=1}^{2} B(\mathbf{r}_i, R_i + \delta_3)$ consists of a single point $\mathbf{p}$ on the triangle connecting $\mathbf{r}_1$ and $\mathbf{r}_2$ with distance $R_1 + \delta_3$ and $R_2 + \delta_3$ to $\mathbf{r}_1$ and $\mathbf{r}_2$, respectively. If $\delta_3 = \delta_{\max}$, then the triple intersection $\cap_{i=1}^{3} B(\mathbf{r}_i, R_i + \delta_{\max})$ is non-empty and contained in the double intersection $\cap_{i=1}^{2} B(\mathbf{r}_i, R_i + \delta_{\max}) = \{\mathbf{p}\}$, therefore the triple intersection is the singleton $\{\mathbf{p}\}$ and the point $\mathbf{p}$ must satisfy (4.6). $\square$

Lemma 4.3. If $\delta_{\max} > \delta_3 = \max(\delta_1, \delta_2, \delta_3)$, then the triple intersection $\cap_{i=1}^{3} B(\mathbf{r}_i, R_i + \delta_{\max})$ at maximal shell radius $\delta = \delta_{\max}$ consists of a single point $\mathbf{p}$ that lies in the interior of the triangle $\mathcal{T}$ and satisfies

$$|\mathbf{p} - \mathbf{r}_i| = R_i + \delta_{\max}, \quad i = 1, 2, 3. \tag{4.7}$$

Therefore the circle $\partial B(\mathbf{p}, \delta_{\max})$ is tangent to each of the circles $\partial B(\mathbf{r}_i, R_i)$ (i.e., it intersects each of those circles in exactly one point): it is one of the circles that solves the Apollonius problem.

Proof. For $\delta > \delta_3$, the pairwise intersection $\mathcal{L}_{pc}(\delta) := B(\mathbf{r}_1, R_1 + \delta) \cap B(\mathbf{r}_2, R_2 + \delta)$ of two disks is a lens-shaped non-empty, compact, convex set. The intersection of the lens with $B(\mathbf{r}_3, R_3 + \delta)$ is equal to the triple intersection of the disks $B(\mathbf{r}_i, R_i + \delta)$, $i = 1, 2, 3$. It is empty for $\delta < \delta_{\max}$ and non-empty for $\delta \ge \delta_{\max}$. Therefore, for $\delta < \delta_{\max}$, the lens $\mathcal{L}_{pc}(\delta)$ has distance strictly larger than $R_3 + \delta$ to $\mathbf{r}_3$; for $\delta = \delta_{\max}$, the lens has distance equal to $R_3 + \delta_{\max}$ to $\mathbf{r}_3$. Let $\mathbf{p}$ be the uniquely defined point on the boundary of the lens that minimizes the distance towards $\mathbf{r}_3$, so that $|\mathbf{p} - \mathbf{r}_3| = R_3 + \delta_{\max}$. Then

$$\bigcap_{i=1}^{3} B(\mathbf{r}_i, R_i + \delta_{\max}) = \mathcal{L}_{pc}(\delta_{\max}) \cap B(\mathbf{r}_3, R_3 + \delta_{\max}) = \{\mathbf{p}\}. \tag{4.8}$$

The point $\mathbf{p}$ lies on the boundary of the lens, therefore $|\mathbf{p} - \mathbf{r}_i| \le R_i + \delta_{\max}$ for $i = 1, 2$ with equality in at least one of the indices 1,2. Suppose by contradiction that equality holds for exactly one index, say $|\mathbf{p} - \mathbf{r}_2| = R_2 + \delta_{\max}$ but $|\mathbf{p} - \mathbf{r}_1| < R_1 + \delta_{\max}$. This means that $\mathbf{p}$ is not a corner of the lens. Then $\mathbf{p}$ must be on the intersection of $\partial B(\mathbf{r}_2, R_2 + \delta_{\max})$ with the segment $[\mathbf{r}_2, \mathbf{r}_3]$. This implies $\delta_{\max} = \delta_1$, contradicting the assumption $\delta_{\max} > \max(\delta_1, \delta_2, \delta_3)$. Therefore $\mathbf{p}$ is a corner of the lens and $|\mathbf{p} - \mathbf{r}_i| = R_i + \delta_{\max}$ for all $i \in \{1, 2, 3\}$.

Finally, suppose by contradiction that the lens corner $\mathbf{p}$ is not in the interior of the triangle. If it is on the boundary, then it must be on the triangle side connecting $\mathbf{r}_1$ and $\mathbf{r}_3$, hence $\delta_{\max} = \delta_2$ in contradiction with $\delta_{\max} > \delta_3 \ge \delta_2$. If $\mathbf{p}$ is outside $\mathcal{T}$, then the lens must contain a part of the segment $[\mathbf{r}_1, \mathbf{r}_3]$ in its interior. The intersection of $\partial B(\mathbf{r}_1, R_1 + \delta_{\max})$ with the segment consists of a single point $\mathbf{q}$ that is closer to $\mathbf{r}_3$ than $\mathbf{p}$, contradicting the definition of $\mathbf{p}$. $\square$

The following is a converse to the previous Lemma.

Lemma 4.4. Suppose that there exist a point $\mathbf{p}$ in the interior of the triangle $\mathcal{T}$ and a radius $\delta^* > 0$ such that $|\mathbf{p} - \mathbf{r}_i| = R_i + \delta^*$ for $i = 1, 2, 3$. Then $\delta_{\max}$ is equal to δ^* and the triple intersection of the disks $B(\mathbf{r}_i, R_i + \delta_{\max})$ consists of the unique point $\mathbf{p}$.

Proof. The point $\mathbf{p}$ is in the triple intersection $\cap_{i=1}^{3} B(\mathbf{r}_i, R_i + \delta^*)$, therefore the latter is non-empty and $\delta_{\max} \le \delta^*$. At $\delta = \delta^*$, the double intersections $\mathcal{L}_{ij}(\delta) = \cap_{s \in \{i,j\}} B(\mathbf{r}_s, R_s + \delta)$ are lens-shaped regions, centered on the triangle sides, that meet at their tips in $\mathbf{p}$, so the triple intersection consists of exactly the point $\mathbf{p}$. At $\delta < \delta^*$ the lenses are smaller and do not meet at all, hence the triple intersection is empty and $\delta_{\max}$ is actually equal to δ^*. $\square$

Proposition 4.1 follows from Lemmas 4.2–4.4, the details are left to the reader.

B. Monotonicity. Proof of Proposition 3.8

Let us investigate how the maximal shell radius $\delta_{\max}$ changes when we vary the angle α_1 at fixed side lengths ℓ_2 and ℓ_3 (without loss of generality). We distinguish three cases:

1. $\delta_{\max} = \max(\delta_2, \delta_3)$, i.e., we are in case 2 of Proposition 4.1 with triple intersection point on one of the triangle sides adjacent to $\mathbf{r}_1$.
2. $\delta_{\max} = \delta^* > \max(\delta_1, \delta_2, \delta_3)$ with triple intersection point in the interior of the triangle (case 1 of Proposition 4.1).
3. $\delta_{\max} = \delta_1$, i.e., triple intersection point on the triangle edge opposite $\mathbf{r}_1$ (back to case 2 of Proposition 4.1).

We shall see in Steps 4–5 below that, as α_1 increases, the cases occur in the order listed above. That is, for small α_1 the point of triple intersection may be initially on one of the triangle sides adjacent to $\mathbf{r}_1$ and stay there for small α_1. With increasing α_1 the point moves to the interior of the triangle until it hits the side opposite $\mathbf{r}_1$; once there, it does not leave.

The proof of Proposition 3.8 is in several steps. First we establish monotonicity within the three cases (steps 1–3), then we address the order of occurrence of the three cases (steps 4–5), and finally we conclude using Proposition 4.1.

1. Monotonicity within case 1 is trivial as δ_2 and δ_3 do not depend on α_1.
2. Monotonicity within case 3 is easily established as well. The threshold $\delta_1 = \frac{1}{2}(\ell_1 - R_2 - R_3)$ depends on α_1 via ℓ_1 given by

$$\ell_1^2 = \ell_2^2 + \ell_3^2 - 2\ell_2\ell_3 \, \cos\alpha_1. \tag{4.9}$$

   Hence ℓ_1 and $\delta_1 = \delta_1(\alpha_1)$ are increasing functions of $\alpha_1 \in (0, \pi)$.
3. For monotonicity within case 2 of the list above, let $\mathbf{p}$ be the triple intersection point in the interior of the triangle. The ray from $\mathbf{r}_1$ to $\mathbf{p}$ splits the angle $\alpha_1 \in (0, \pi)$ into two angles $\alpha_1^{(2)} > 0$ and $\alpha_1^{(3)} > 0$ (see Fig. 3),

$$\alpha_1 = \alpha_1^{(2)} + \alpha_1^{(3)}. \tag{4.10}$$

By the cosine rule in the triangle with vertices $\mathbf{r}_1, \mathbf{r}_2, \mathbf{p}$, the angle $\alpha_1^{(2)}$ satisfies

$$\cos\left(\alpha_1^{(2)}\right) = \frac{\ell_3^2 + (R_2 + \delta^*)^2 - (R_1 + \delta^*)^2}{2\ell_3(R_1 + \delta^*)} =: f_2(\delta^*) \tag{4.11}$$

Similarly,

$$\cos\left(\alpha_1^{(3)}\right) = \frac{\ell_2^2 + (R_3 + \delta^*)^2 - (R_1 + \delta^*)^2}{2\ell_2(R_1 + \delta^*)} =: f_3(\delta^*). \tag{4.12}$$

The derivative of the right-hand side of (4.11) with respect to δ^* (at fixed R_1, R_2 and ℓ_3) can be computed explicitly, it is equal to

$$f_2'(\delta^*) = \frac{(R_1 - R_2)^2 - \ell_3^2}{2\ell_3(R_1 + \delta^*)} < 0. \tag{4.13}$$

It is strictly negative because $\ell_3 \geq R_1 + R_2 > |R_1 - R_2|$. Furthermore $f_2(\delta_3) = 1$ and

$$\lim_{\delta^* \to \infty} f_2(\delta^*) = \frac{R_2 - R_1}{\ell_3} \in (-1, 1). \tag{4.14}$$

It follows that the solution to Eq. (4.11), given by

$$\alpha_1^{(2)}(\delta^*) := \arccos f_2(\delta^*) \in [0, \pi) \quad (\delta^* \geq \delta_3) \tag{4.15}$$

is a strictly increasing function of δ^*. The same holds true for

$$\alpha_1^{(3)}(\delta^*) := \arccos f_3(\delta^*) \in [0, \pi) \quad (\delta^* \geq \delta_2). \tag{4.16}$$

Therefore Eqs. (4.10)–(4.12) determine the angle α_1 uniquely as a strictly increasing function of δ^*. Inverting the relationship, we see that $\delta^* = \delta^*(\alpha_1)$ is an increasing function of α_1. Monotonicity within case 2 of the list above follows.

4. Now we turn to the order in which the cases occur. We may assume without loss of generality $\delta_3 \geq \delta_2$. Let $\mathbf{q}$ be the point of contact of $B(\mathbf{r}_1, R_1)$ and $B(\mathbf{r}_2, R_2)$. Then case 1 occurs if and only if $|\mathbf{q} - \mathbf{r}_3| \leq R_3 + \delta_3$. Because of

$$|\mathbf{q} - \mathbf{r}_3|^2 = (R_1 + \delta_3)^2 + \ell_2^2 - 2(R_1 + \delta_3)\ell_2 \, \cos\alpha_1, \tag{4.17}$$

the distance $|\mathbf{q} - \mathbf{r}_3|$ increases with α_1. Therefore, once $|\mathbf{q} - \mathbf{r}_3|$ crosses the threshold $R_3 + \delta_3$ it stays above the threshold. That is, once we have left case 1 we do not come back to it.

5. Similarly, once we leave case 2 while increasing α_1, we do not come back to it. To see why, we revisit the computations from step 3. Let $\alpha_1 \in (0, \pi)$ be an angle that falls into case 2. Then, as proven earlier, $\delta_{\max}(\alpha_1) = \delta^*(\alpha_1)$ is a solution to Eqs. (4.10)–(4.12). Moreover, because the center $\mathbf{p}$ of the circle $\partial B(\mathbf{p}, \delta^*)$ is inside the triangle $\mathcal{T}$, the inner angle β_1 at $\mathbf{p}$ in the triangle with vertices $\mathbf{p}, \mathbf{r}_2, \mathbf{r}_3$ is smaller than π. The angle $\beta_1 = \beta_1(\alpha_1)$ is an increasing function of α_1. This is because the angles $\alpha_2^{(1)}$ and $\alpha_3^{(1)}$ are increasing functions of δ^*, by arguments similar to step 3, and

$$\beta_1 = 2\pi - \alpha_1 - \alpha_2^{(1)} - \alpha_3^{(1)}. \tag{4.18}$$

Conversely, let α_1 be an angle with $\alpha_1 = \alpha_1^{(2)}(\delta^*) + \alpha_1^{(3)}(\delta^*) =: \alpha_1(\delta^*)$ for some $\delta^* > \max(\delta_2, \delta_3)$, with $\alpha_1^{(i)}(\delta^*)$ defined as in Eqs. (4.15) and (4.16). The angles $\alpha_1^{(i)}(\delta^*)$ allow us to set a point $\mathbf{q}$ that satisfies $|\mathbf{q} - \mathbf{r}_i| = R_i + \delta^*$ for $i = 1, 2, 3$. In general the point $\mathbf{q}$ might be outside the triangle or on its boundary, but if $\beta_1 < \pi$, then the point $\mathbf{q}$ is in the interior of the triangle and we are in case 2.

Fix an angle α_1 that falls within case 3 and pick $\alpha_1' > \alpha_1$. We want to show that α_1' falls into case 3 as well. By step 4 we know that α_1' cannot fall into case 1, it remains to exclude case 2. The map $\delta^* \mapsto \alpha_1(\delta^*)$ is a strictly increasing bijection from $[\max(\delta_2, \delta_3), \infty]$ onto some subinterval of $(0, \infty)$. Therefore, if the equation $\alpha_1(\delta^*) = \alpha_1$ has no solution, the same holds true for all $\alpha_1' > \alpha_1$ and α_1' cannot fall into case 2. If the equation $\alpha_1(\delta^*) = \alpha_1$ has a solution, then by the considerations above we must have $\beta_1(\alpha_1) \geq \pi$ hence $\beta_1(\alpha_1') \geq \beta_1(\alpha_1) \geq \pi$ and case 2 is excluded as well. Thus we have proven that if α_1 is in case 3, then all larger angles $\alpha_1' \geq \alpha_1$ are in case 3 as well.

6. The monotonicity of the map $\alpha_1 \mapsto \delta_{\max}(\alpha_1, \ell_2, \ell_3)$ and, generally, $\alpha_i \mapsto \delta_{\max}(\alpha_i, \ell_j, \ell_k)$ follows from Steps 1–5 and the continuity of the map.

$\square$

C. Descartes' circle theorem. Proof of Proposition 3.10

Consider three circles with centers $\mathbf{r}_i$ and radii $R_i > 0$ that are in contact, i.e., $\ell_1 = R_2 + R_3$ and similarly for the other triplets. In this situation the pairwise thresholds δ_i vanish and in view of $\delta_{\max} > 0$, we are automatically in case 1 of Proposition 4.1.

Thus $\delta_{\max} = \delta^*$ is the radius of a circle $\partial B(\mathbf{p}, \delta^*)$ centered in the interior of the triangle and tangent to the three adjacent circles $\partial B(\mathbf{r}_i, R_i)$.

This is precisely the special case of the Apollonius problem addressed by Descartes' circle theorem. There are exactly two circles adjacent to the three circles $\partial B(\mathbf{r}_i, R_i)$. There always exists one solution circle which is inscribed inside the void delimited by the three given circles while the other solution circle either contains all three of them [bottom panel of Fig. 2(a)] or forms a void together with two of the given circles containing the third one [bottom panel of Fig. 2(b)]. Clearly the solution that interests us is the inner circle, called inner Soddy circle. Its radius is known (see for example[65,66]), it is equal to the expression for $\delta_{\mathrm{cr}}(R_1, R_2, R_3)$ given in Proposition 3.10. This completes the proof of the proposition.

$\square$

V. SUMMARY AND PHYSICAL INTERPRETATION OF GEOMETRIC CRITERIA

To summarize, we have established rigorous geometric criteria for the absence of many-body interactions higher than pairwise in AO-type mixtures involving hard colloids and ideal depletants in any spatial dimension. Once the stated criteria are obeyed, our results imply that the depletants can be integrated out and there exists an exact mapping onto a system with effective pairwise interactions only. Mathematically, the absence of triplet and N-body interactions with $N \geq 3$ in a fluid of hard bodies for a given depletion radius is equivalent to the triple intersection of the corresponding dilated bodies (and thus also the intersections between more than three dilated bodies) having zero volume for any possible configuration of the hard bodies. We elucidated relevant conditions for this problem in Theorems 3.2 and 3.3 and proved them with elementary geometry.

For the exactness of the depletion interaction between *identical colloidal hard spheres*, the sufficient and necessary geometric criterion, Eq. (2.6), was already stated in the literature but is mathematically proven here as a special case of Eq. (3.4) with all radii being equal, i.e., for $R = R_1 = R_2 = R_3$.

The generalized condition in our Theorem 3.3 holds for *polydisperse mixtures of hard spheres* in any spatial dimension, where the radius $R = \min_i R_i$ of the smallest species sets the threshold according to Eq. (3.4).

Moreover, we provide a condition, Eq. (3.2), which is sufficient for the exactness of the pairwise depletion interaction between *convex hard particles*, also including *polydisperse mixtures* thereof. The generalized upper bound for the depletion radius provided in Theorem 3.2 is proportional to the minimal rolling radius among all bodies, which corresponds to the curvature radius at the point on the surface of any body which has the largest curvature. This criterion may, however, turn out to be extremely susceptible to irregularities of the surface geometry (a detailed discussion can be found below in Sec. VI). We therefore note that a systematic improvement of the threshold in Eq. (3.2) can be achieved, along the lines of Proposition 3.5, by applying Theorem 3.2 to appropriately chosen auxiliary bodies (with larger rolling radii) that are contained in the original bodies.

By slightly reformulating our main theorems, we also address the problem of effective depletion interactions between *arbitrarily-shaped convex particles and a planar hard wall* in Theorem 3.11. In this case, a one-body depletion potential can be found from integrating out the

depletants. Such a potential is exact if there are no effective pair and N-body interactions with $N \geq 2$, which is again equivalent to the triple intersection of the corresponding dilated bodies (including that of the wall) having zero volume. The sufficient and necessary geometric criterion, Eq. (2.7), for identical spheres has been generalized to Eq. (3.19), which again shows that the radius of the smallest species determines the critical depletion radius for polydisperse mixtures of hard spheres. Relatedly, Eq. (3.18) provides a sufficient criterion for general polydisperse mixtures based on the minimal occurring curvature radius.

Although not explicitly stated in our theorems, our mathematical analysis directly applies to *polydisperse spherical depletants*, for which the depletion radius $\delta^{(v)}$ may depend on the species v. In this case, our criteria should be interpreted to provide thresholds for the maximal depletion radius $\delta = \max_v \delta^{(v)}$ associated with the "largest" depletant species.

Non-spherical depletants such as needles or rods, which have been widely considered in the literature,[68–74] give rise to a nonspherical shape of the depletion shell which depends on their orientation. The thresholds for δ can thus directly be applied as sufficient criteria on the maximal radius of such a generalized depletion shell.

In some of the above cases a better upper bound could be found upon considering the resulting generalized geometric overlap problem in its full complexity. To do so, the basic mathematical framework built up for establishing the presented criteria serves as a convenient starting point, as exemplified in Proposition 3.5.

VI. CONCLUSIONS

Let us conclude with a couple of remarks regarding the broader physical implications of our criteria and possible generalizations.

First of all, if the convex colloidal particles have a *cusp* in their shape, like colloidal polyhedra,[75,76] our sufficient criteria become trivial since the rolling radius vanishes (diverging local surface curvature). The resulting condition $\delta < 0$ can never be fulfilled by a positive depletion radius δ, such that the absence of higher-body depletion interactions can never be guaranteed. Indeed, many regular particle shapes, e.g., tetrahedral or cubic, can arrange in configurations with the cusps of three or more particles at direct contact. In these special cases, it is apparent that any choice of depletion radius $\delta > 0$ results in overlapping depletion shells, so that our criteria even become necessary. In contrast, if configurations with three touching cusps are forbidden, e.g., for particles with sufficiently large opening angles, the formal condition $\delta < 0$ apparently is no longer sharp. This extreme example illustrates that the maximal depletion radius can strongly depend on the particle shape. In practice, this is also relevant for colloidal particles, which are always slightly rounded.[75] Regarding the convenient possibility to approximate the shape of smooth bodies by appropriate polygons, particles with cusps do indeed remain relevant for theoretical treatments. In both cases of singular cusps or smooth irregularities of the surface, an improved sufficient bound can be implicitly specified according to Proposition 3.5. The open question of whether this criterion is also necessary remains an interesting problem for future work.

Second, *non-convex* hard bodies play an important role in modeling lock-and-key colloids[77,78] where the depletion attraction has been used as a bonding mechanism.[77,79] Other relevant nonconvex shapes are clusters of spheres firmly attached to each other by surface chemistry,[80,81] colloidal bowls[79,82,83] or even more general objects, see Ref. 84 for some examples. As stated in Remark 3.4, our sufficient criteria do also apply for nonconvex shapes. However, the provided thresholds could, in principle, become arbitrarily poor, imagining, for example particles possessing a cusp which is inaccessible to other particles. Therefore, we leave an improvement of our bounds for such particles to future studies.

Third, another important problem which we did not explicitly consider here is the depletion at *curved hard walls*. In the case of externally placed obstacles,[36] which provide a model for a porous medium, a criterion for the absence of effective external pair interactions can be found analogously to case of a planar hard wall by considering Eq. (3.17) without sending the wall radius R_w to infinity. We further expect that the structure of our proof can also be applied to rigorously determine an explicit formula for the critical depletion radius for a fluid in external hard-body confinement.[37] In this case, we expect that such a threshold is related to a solution of the Apollonius problem involving internal tangency.

Fourth, one may consider more realistic situations of *softened colloid–polymer interactions*[85,86] or non-vanishing polymer–polymer interactions.[85,87] Only for colloid–polymer interactions which exhibit a sharp exclusion zone of radius δ plus an interaction of strict finite range ϵ and for ideal polymers, the pure geometric concept applies such that our criteria can be used for the overall range $\delta + \epsilon$ of the colloid–polymer interaction. Long-ranged colloid–polymer interactions will induce many-body interactions even for ideal polymers. Likewise, non-vanishing polymer–polymer interactions will in general contribute to many-body interactions of any order due to their finite correlation length.

Fifth, recent studies have included *activity* in the depletants leading to active depletion interaction between colloids.[88–91] For ideal active depletants, the generalization of the AO pair interaction was computed recently[91] using the concept of swim pressure. It is important to mention here that our proof for the absence of many-body interactions does also apply to active ideal depletants, as the basic geometric conditions are identical. The only difference is that for active depletants the osmotic swim pressure depends on the shape and local curvature of the excluded zone but this only affects the strength of the pair interactions but not the geometric conditions for triple intersection. On a further note, the effective interactions between active colloids display intriguing similarities with effective depletion interactions[92] but are generally of intrinsic many-body nature.[92–96]

Finally, beyond verifying the absence of effective triplet interactions in the AO model, the *magic number* $2/\sqrt{3} - 1 \approx 0.1547$ is in fact a more general indicator of crossover behavior in hard-particle systems. For example, the close-packing density in a binary mixture of hard spheres changes its behavior as a function of the size ratio around this value.[97] When the size ratio is below this threshold, there even exist

dynamical escape routes for the smaller particles preventing their vitrification.[98] Our presented ideas could thus be also helpful to deepen the mathematical understanding of such related physical problems.

ACKNOWLEDGMENTS

AUTHOR DECLARATIONS

Conflict of Interest

The authors have no conflicts of interest to disclose.

Author Contributions

René Wittmann: Conceptualization (equal); Formal analysis (equal); Funding acquisition (equal); Methodology (equal); Project administration (equal); Validation (equal); Visualization (lead); Writing – original draft (lead); Writing – review & editing (equal). **Sabine Jansen**: Conceptualization (equal); Formal analysis (equal); Funding acquisition (equal); Methodology (equal); Validation (equal); Visualization (supporting); Writing – original draft (supporting); Writing – review & editing (equal). **Hartmut Löwen**: Conceptualization (lead); Funding acquisition (equal); Project administration (equal); Supervision (lead); Validation (equal); Writing – original draft (supporting); Writing – review & editing (equal).

DATA AVAILABILITY

The data that support the findings of this study are available within the article.

REFERENCES

[1] P. Ballone, G. Pastore, G. Galli, and D. Gazzillo, "Additive and non-additive hard sphere mixtures: Monte Carlo simulation and integral equation results," Mol. Phys. **59**, 275–290 (1986).

[2] M. Dijkstra, "Phase behavior of nonadditive hard-sphere mixtures," Phys. Rev. E **58**, 7523 (1998).

[3] M. Dijkstra, R. van Roij, and R. Evans, "Direct simulation of the phase behavior of binary hard-sphere mixtures: Test of the depletion potential description," Phys. Rev. Lett. **82**, 117 (1999).

[4] R. Roth and R. Evans, "The depletion potential in non-additive hard-sphere mixtures," Europhys. Lett. (EPL) **53**, 271 (2001).

[5] M. Schmidt, H. Löwen, J. M. Brader, and R. Evans, "Density functional for a model colloid-polymer mixture," Phys. Rev. Lett. **85**, 1934–1937 (2000).

[6] M. Schmidt, H. Löwen, J. M. Brader, and R. Evans, "Density functional theory for a model colloid polymer mixture: Bulk fluid phases," J. Phys.: Condens. Matter **14**, 9353 (2002).

[7] M. Schmidt, "Rosenfeld functional for non-additive hard spheres," J. Phys.: Condens. Matter **16**, L351 (2004).

[8] P. Hopkins and M. Schmidt, "Binary non-additive hard sphere mixtures: Fluid demixing, asymptotic decay of correlations and free fluid interfaces," J. Phys.: Condens. Matter **22**, 325108 (2010).

[9] C. D. Estrada-Alvarez, E. López-Sánchez, G. Pérez-Ángel, P. González-Mozuelos, J. M. Méndez-Alcaraz, and R. Castañeda-Priego, "Note: Depletion potentials in non-additive asymmetric binary mixtures of hard-spheres," J. Chem. Phys. **140**, 026101 (2014).

[10] S. Lin and M. Oettel, "Phase diagrams and crystal-fluid surface tensions in additive and nonadditive two-dimensional binary hard-disk mixtures," Phys. Rev. E **98**, 012608 (2018).

[11] E. Fayen, A. Jagannathan, G. Foffi, and F. Smallenburg, "Infinite-pressure phase diagram of binary mixtures of (non) additive hard disks," J. Chem. Phys. **152**, 204901 (2020).

[12] S. A. Egorov, "Phase behavior of colloid-polymer mixtures in planar, spherical, and cylindrical confinement: A density functional theory study," J. Chem. Phys. **154**, 184902 (2021).

[13] N. Ditz and R. Roth, "Gas–liquid phase transition in a binary mixture with an interaction that creates constant density profiles," J. Chem. Phys. **154**, 204905 (2021).

[14] P. N. Pusey, in *Liquids, Freezing and the Glass Transition*, edited by J. P. Hansen, D. Levesque, and J. Zinn-Justin (North-Holland, Amsterdam, 1991).

[15] H. N. W. Lekkerkerker and R. Tuinier, "Depletion interaction," in *Colloids and the Depletion Interaction* (Springer, 2011), pp. 57–108.

[16] W. C. K. Poon, "The physics of a model colloid polymer mixture," J. Phys.: Condens. Matter **14**, R859 (2002).

[17] S. M. Liddle, T. Narayanan, and W. C. K. Poon, "Polydispersity effects in colloid–polymer mixtures," J. Phys.: Condens. Matter **23**, 194116 (2011).

[18] J. Opdam, M. P. M. Schelling, and R. Tuinier, "Phase behavior of binary hard-sphere mixtures: Free volume theory including reservoir hard-core interactions," J. Chem. Phys. **154**, 074902 (2021).

[19] A. R. Denton and W. J. Davis, "Influence of solvent quality on depletion potentials in colloid–polymer mixtures," J. Chem. Phys. **155**, 084904 (2021).

[20] F. Gußmann, H. Hansen-Goos, S. Dietrich, and R. Roth, "Liquid–liquid phase separation in an inhomogeneous ternary colloid–polymer mixture," J. Chem. Phys. **154**, 224504 (2021).

[21] A. M. Tom, W. K. Kim, and C. Hyeon, "Polymer brush-induced depletion interactions and clustering of membrane proteins," J. Chem. Phys. **154**, 214901 (2021).

[22] M. Gimperlein and M. Schmiedeberg, "Structural and dynamical properties of dilute gel networks in colloid–polymer mixtures," J. Chem. Phys. **154**, 244903 (2021).

[23] F. Oosawa and S. Asakura, "Surface tension of high-polymer solutions," J. Chem. Phys. **22**, 1255 (1954).

[24] S. Asakura and F. Oosawa, "On interaction between two bodies immersed in a solution of macromolecules," J. Chem. Phys. **22**, 1255–1256 (1954).

[25] K. Miyazaki, K. S. Schweizer, D. Thirumalai, R. Tuinier, and E. Zaccarelli, "The Asakura–Oosawa theory: Entropic forces in physics, biology, and soft matter," J. Chem. Phys. **156**, 080401 (2022).

[26] F. Oosawa, "The history of the birth of the Asakura–Oosawa theory," J. Chem. Phys. **155**, 084104 (2021).

[27] A. Vrij, "Polymers at interfaces and the interactions in colloidal dispersions," Pure Appl. Chem. **48**, 471–483 (1976).

[28] J. P. Hansen and H. Löwen, "Effective interactions for large-scale simulations of complex fluids," in *Bridging Time Scales: Molecular Simulations for the Next Decade* (Springer, 2002), pp. 167–196.

[29] M. Dijkstra, R. van Roij, R. Roth, and A. Fortini, "Effect of many-body interactions on the bulk and interfacial phase behavior of a model colloid-polymer mixture," Phys. Rev. E **73**, 041404 (2006).

[30] M. Maeritz and M. Oettel, "Density functional for the lattice gas from fundamental measure theory," Phys. Rev. E **104**, 024124 (2021).

[31] M. Maeritz and M. Oettel, "Droplet condensation in the lattice gas with density functional theory," Phys. Rev. E **104**, 034127 (2021).

[32] J. S. Rowlinson and B. Widom, *Molecular Theory of Capillarity* (Courier Corporation, 2013).

[33] J. M. Brader, M. Dijkstra, and R. Evans, "Inhomogeneous model colloid-polymer mixtures: Adsorption at a hard wall," Phys. Rev. E **63**, 041405 (2001).

[34] R. Evans, J. M. Brader, R. Roth, M. Dijkstra, M. Schmidt, and H. Löwen, "Interfacial properties of model colloid–polymer mixtures," Philos. Trans. R. Soc., A **359**, 961–975 (2001).

[35] J. M. Brader, R. Evans, M. Schmidt, and H. Löwen, "Entropic wetting and the fluid-fluid interface of a model colloid-polymer mixture," J. Phys.: Condens. Matter **14**, L1 (2001).

[36] P. P. F. Wessels, M. Schmidt, and H. Löwen, "Wetting, drying, and layering of colloid-polymer mixtures at porous interfaces," Phys. Rev. Lett. **94**, 078303 (2005).

[37] A. Winkler, A. Statt, P. Virnau, and K. Binder, "Phase transitions and phase equilibria in spherical confinement," Phys. Rev. E **87**, 032307 (2013).

[38] K. Binder, P. Virnau, and A. Statt, "Perspective: The Asakura–Oosawa model: A colloid prototype for bulk and interfacial phase behavior," J. Chem. Phys. **141**, 140901 (2014).

[39] J. Glaser, A. S. Karas, and S. C. Glotzer, "A parallel algorithm for implicit depletant simulations," J. Chem. Phys. **143**, 184110 (2015).

[40] J. A. Wood, Y. Liu, and A. Widmer-Cooper, "Crystal nucleation in colloidal rod suspensions: The effect of depletant size," J. Chem. Phys. **154**, 244505 (2021).

[41] V. F. D. Peters, M. Vis, R. Tuinier, and H. N. W. Lekkerkerker, "Phase separation in mixed suspensions of bacteria and nonadsorbing polymers," J. Chem. Phys. **154**, 151101 (2021).

[42] T. G. Mason, "Depletion torques between anisotropic colloidal particles," J. Chem. Phys. **155**, 144903 (2021).

[43] R. Cheng, J. Li, I. Ríos de Anda, T. W. C. Taylor, M. A. Faers, J. L. R. Anderson, A. M. Seddon, and C. P. Royall, "Protein–polymer mixtures in the colloid limit: Aggregation, sedimentation, and crystallization," J. Chem. Phys. **155**, 114901 (2021).

[44] C. Calero, M. Díaz-Morata, and I. Pagonabarraga, "Aggregation of discoidal particles due to depletion interaction," J. Chem. Phys. **155**, 074904 (2021).

[45] N. M. de Los Santos-López, G. Pérez-Ángel, J. M. Méndez-Alcaraz, and R. Castañeda-Priego, "Competing interactions in the depletion forces of ternary colloidal mixtures," J. Chem. Phys. **155**, 024901 (2021).

[46] A. Kuhnhold and P. van der Schoot, "Structure of nematic tactoids of hard rods," J. Chem. Phys. **156**, 104501 (2022).

[47] A. P. Gast, W. B. Russel, and C. K. Hall, "An experimental and theoretical study of phase transitions in the polystyrene latex and hydroxyethylcellulose system," J. Colloid Interface Sci. **109**, 161–171 (1986).

[48] M. Dijkstra, J. M. Brader, and R. Evans, "Phase behaviour and structure of model colloid-polymer mixtures," J. Phys.: Condens. Matter **11**10079 (1999).

[49] J. M. Brader, R. Evans, and M. Schmidt, "Statistical mechanics of inhomogeneous model colloid—Polymer mixtures," Mol. Phys. **101**, 3349–3384 (2003).

[50] H. Löwen and E. Allahyarov, "The role of effective triplet interactions in charged colloidal suspensions," J. Phys.: Condens. Matter **10**, 4147 (1998).

[51] A. Moncho-Jordá, A. A. Louis, P. G. Bolhuis, and R. Roth, "The Asakura–Oosawa model in the protein limit: The role of many-body interactions," J. Phys.: Condens. Matter **15**, S3429 (2003).

[52] C. Russ, M. Brunner, C. Bechinger, and H. H. von Grünberg, "Three-body forces at work: Three-body potentials derived from triplet correlations in colloidal suspensions," Europhys. Lett. (EPL) **69**, 468 (2005).

[53] A. Santos, M. Lopez de Haro, G. Fiumara, and F. Saija, "The effective colloid interaction in the Asakura–Oosawa model. assessment of non-pairwise terms from the virial expansion," J. Chem. Phys. **142**, 224903 (2015).

[54] H. Kobayashi, P. Rohrbach, R. Scheichl, N. B. Wilding, and R. L. Jack, "Correction of coarse-graining errors by a two-level method: Application to the Asakura–Oosawa model," J. Chem. Phys. **151**, 144108 (2019).

[55] G. Campos-Villalobos, E. Boattini, L. Filion, and M. Dijkstra, "Machine learning many-body potentials for colloidal systems," J. Chem. Phys. **155**, 174902 (2021).

[56] J. P. Hansen and I. R. McDonald, *Theory of Simple Liquids* (Elsevier, 1990).

[57] T. C. Hales, "A proof of the Kepler conjecture," Ann. Math. **162**, 1065–1185 (2005).

[58] M. Baake and U. Grimm, *Aperiodic Order*, Encyclopedia of Mathematics and Its Applications (Cambridge University Press, Cambridge, NY, 2013).

[59] W. Blaschke, *Kreis und Kugel* (Walter de Gruyter & Co., Berlin, 1956).

[60] R. Howard, "Blaschke's rolling theorem for manifolds with boundary," Manuscripta Math. **99**, 471–483 (1999).

[61] V. Bangert, "Convex hypersurfaces with bounded first mean curvature measure," Calculus Var. Partial Differ. Equations **8**, 259–278 (1999).

[62] D. Hug, *Measures, Curvatures and Currents in Convex Geometry* (Habilitationsschrift; Albert-Ludwigs-Universität, Freiburg, 1999).

[63] D. Hug, "Absolute continuity for curvature measures of convex sets, III," Adv. Math. **169**, 92–117 (2002).

[64] F. Soddy, "The kiss precise," Nature **137**, 1021 (1936).

[65] H. S. M. Coxeter, "The problem of Apollonius," Am. Math. Mon. **75**, 5–15 (1968).

[66] A. Oldknow, "The Euler-Gergonne-Soddy triangle of a triangle," Am. Math. Mon. **103**, 319–329 (1996).

[67] R. A. Johnson, in *Advanced Euclidean Geometry: An Elementary Treatise on the Geometry of the Triangle and the Circle*, edited by J. W. Young (Dover Publications, Inc., New York, 1960).

27 October 2023 11:53:56

[68] Y. Mao, M. E. Cates, and H. N. W. Lekkerkerker, "Depletion stabilization by semidilute rods," Phys. Rev. Lett. **75**, 4548 (1995).

[69] Y. Mao, M. E. Cates, and H. N. W. Lekkerkerker, "Theory of the depletion force due to rodlike polymers," J. Chem. Phys. **106**, 3721–3729 (1997).

[70] Y.-L. Chen and K. S. Schweizer, "Depletion interactions in suspensions of spheres and rod–polymers," J. Chem. Phys. **117**, 1351–1362 (2002).

[71] P. R. Lang, "Depletion interaction mediated by polydisperse rods," J. Chem. Phys. **127**, 124906 (2007).

[72] D. Müller, T. A. Kampmann, and J. Kierfeld, "Chaining of hard disks in nematic needles: Particle-based simulation of colloidal interactions in liquid crystals," Sci. Rep. **10**, 12718 (2020).

[73] J. Opdam, D. Guu, M. P. M. Schelling, D. G. A. L. Aarts, R. Tuinier, and M. P. Lettinga, "Phase stability of colloidal mixtures of spheres and rods," J. Chem. Phys. **154**, 204906 (2021).

[74] J. Opdam, P. Gandhi, A. Kuhnhold, T. Schilling, and R. Tuinier, "Excluded volume interactions and phase stability in mixtures of hard spheres and hard rods," Phys. Chem. Chem. Phys. **24**, 11820–11827 (2022).

[75] A. V. Petukhov, R. Tuinier, and G. J. Vroege, "Entropic patchiness: Effects of colloid shape and depletion," Curr. Opin. Colloid Interface Sci. **30**, 54–61 (2017).

[76] M. Marechal and H. Löwen, "Density functional theory for hard polyhedra," Phys. Rev. Lett. **110**, 137801 (2013).

[77] S. Sacanna, W. T. M. Irvine, P. M. Chaikin, and D. J. Pine, "Lock and key colloids," Nature **464**, 575–578 (2010).

[78] Y. Wang, Y. Wang, X. Zheng, G.-R. Yi, S. Sacanna, D. J. Pine, and M. Weck, "Three-dimensional lock and key colloids," J. Am. Chem. Soc. **136**, 6866–6869 (2014).

[79] C. Law, D. J. Ashton, N. B. Wilding, and R. L. Jack, "Coarse-grained depletion potentials for anisotropic colloids: Application to lock-and-key systems," J. Chem. Phys. **145**, 084907 (2016).

[80] D. J. Kraft, R. Wittkowski, B. Ten Hagen, K. V. Edmond, D. J. Pine, and H. Löwen, "Brownian motion and the hydrodynamic friction tensor for colloidal particles of complex shape," Phys. Rev. E **88**, 050301 (2013).

[81] J. R. Wolters, J. E. Verweij, G. Avvisati, M. Dijkstra, and W. K. Kegel, "Depletion-induced encapsulation by dumbbell-shaped patchy colloids stabilize microspheres against aggregation," Langmuir **33**, 3270–3280 (2017).

[82] M. Marechal and M. Dijkstra, "Phase behavior and structure of colloidal bowl-shaped particles: Simulations," Phys. Rev. E **82**, 031405 (2010).

[83] K. V. Edmond, T. W. Jacobson, J. S. Oh, G.-R. Yi, A. D. Hollingsworth, S. Sacanna, and D. J. Pine, "Large-scale synthesis of colloidal bowl-shaped particles," Soft Matter **17**, 6176–6181 (2021).

[84] R. Wittkowski and H. Löwen, "Dynamical density functional theory for colloidal particles with arbitrary shape," Mol. Phys. **109**, 2935–2943 (2011).

[85] A. A. Louis, P. G. Bolhuis, E. J. Meijer, and J. P. Hansen, "Polymer induced depletion potentials in polymer-colloid mixtures," J. Chem. Phys. **117**, 1893–1907 (2002).

[86] S. Ramakrishnan, M. Fuchs, K. S. Schweizer, and C. F. Zukoski, "Entropy driven phase transitions in colloid–polymer suspensions: Tests of depletion theories," J. Chem. Phys. **116**, 2201–2212 (2002).

[87] A. I. Chervanyov, "Depletion interaction between colloids mediated by an athermal polymer blend," Phys. Rev. E **97**, 032508 (2018).

[88] D. Ray, C. Reichhardt, and C. J. O. Reichhardt, "Casimir effect in active matter systems," Phys. Rev. E **90**, 013019 (2014).

[89] R. Ni, M. A. Cohen Stuart, and P. G. Bolhuis, "Tunable long range forces mediated by self-propelled colloidal hard spheres," Phys. Rev. Lett. **114**, 018302 (2015).

[90] J. Harder, S. A. Mallory, C. Tung, C. Valeriani, and A. Cacciuto, "The role of particle shape in active depletion," J. Chem. Phys. **141**, 194901 (2014).

[91] F. Smallenburg and H. Löwen, "Swim pressure on walls with curves and corners," Phys. Rev. E **92**, 032304 (2015).

[92] F. Turci and N. B. Wilding, "Phase separation and multibody effects in three-dimensional active Brownian particles," Phys. Rev. Lett. **126**, 038002 (2021).

[93] A. Kaiser, H. Wensink, and H. Löwen, "How to capture active particles," Phys. Rev. Lett. **108**, 268307 (2012).

[94] T. F. Farage, P. Krinninger, and J. M. Brader, "Effective interactions in active Brownian suspensions," Phys. Rev. E **91**, 042310 (2015).

[95] M. Rein and T. Speck, "Applicability of effective pair potentials for active Brownian particles," Eur. Phys. J. E **39**, 84 (2016).

[96] R. Wittmann, C. Maggi, A. Sharma, A. Scacchi, J. M. Brader, and U. Marini Bettolo Marconi, "Effective equilibrium states in the colored-noise model for active matter I. Pairwise forces in the Fox and unified colored noise approximations," J. Stat. Mech. **2017**, 113207.

[97] R. K. McGeary, "Mechanical packing of spherical particles," J. Am. Ceram. Soc. **44**, 513–522 (1961).

[98] J. Bosse and J. S. Thakur, "Delocalization of small particles in a glassy matrix," Phys. Rev. Lett. **59**, 998–1001 (1987).